Utah State University ground-based test facility for study of electronic properties of spacecraft materials

W. Y. Chang, N. Nickles, R. E. Davies, and J. R. Dennison

Physics Department, Utah State University, Logan, Utah

Abstract. Materials used for spacecraft and space structures in near-Earth orbit are subject to severe environmental effects including high vacuum conditions, hot and cold extremes temperature, strongly oxidizing atomic oxygen environments, and high fluxes of energetic electrons, ions, neutrals and photons. Instrumentation developed at Utah State University is designed to simulate, at least to some level, all of these conditions and to study charged particle and photon interactions with spacecraft surfaces. The facilities are particularly well suited to study electron emission as related to spacecraft charging, including secondary and backscattered yields, energy-spectra, and angle-resolved measurements as a function of incident energy, species, and angle. There are capabilities to determine all parameters required for the NASCAP materials database. Specifically, the chamber provides controlled neutral environments, controlled temperatures, electron fluxes, ion fluxes, photon fluxes, and a wide array of neutral and charged particle and photon detectors. In principle, these capabilities can be used simultaneously, allowing study of synergistic effects. Extensive surface science characterization capabilities are also available to fully characterize the samples *in situ*. Details of the instrumentation and representative measurements are presented.

Project Motivation

Spacecraft charging, due to interactions of spacecraft with the surrounding natural space plasma, is known to be the cause of many system anomalies and component failures [*Bedingfield et al*., 1996; *Leach et al*., 1995]. To assist spacecraft designers in mitigating damage from charging effects, NASA, AFOSR, ESA, and RSA have developed extensive sets of engineering tools to predict the extent of charging in various spacecraft environments (for example, NASCAP/LEO, NASCAP/GEO, POLAR, SPENVIS [*Heynderickx et al*., 1999], and ECO-M [*Danilov et al*., 1999]). However, these tools, along with their materials database, are no longer sufficient in more demanding environments (e.g., polar and geosynchronous orbits), for higher power and voltage solar arrays, and for very sensitive modern (high-density, low-current, and low-voltage) electronics [*Hastings and Garrett*, 1996].

Current NASCAP databases lack electronic properties of most spacecraft materials in use (only nine materials are presently incorporated [*Mandell et al*., 1993]) and many new spacecraft bulk materials or coatings need to be characterized. For the next generation of tools (enhanced NASCAP [*Mandell et al.*, 1999]), more detailed material properties must also be incorporated into the databases for use in enhanced models, such as electron induced energy- and angle-resolved electron yields [*Nickles et al*., 1999], environmental degradation and contamination of materials leading to evolution of electronic materials properties which affect spacecraft charging [*Davies and Dennison*, 1997; *Davies and Dennison*, 1999a], incident-angle dependence of electron yields, photon energy dependence of electron yields, and thermal coefficients of electrical conductivity.

Project Description

To ameliorate these concerns, the NASA Space Environments and Effects (NASA/SEE) Program has funded a three year study (July 1998 to July 2001) of electronic properties of spacecraft materials at Utah State University [*Dennison*, 1998]. The project time table is summarized as follows:

Year 1: Measurement of NASCAP parameters for standard conductive materials including elemental conductors, conducting alloys, and conductive coatings.
Year 2: Measurement of NASCAP parameters for standard insulators (bulk and coatings), energy- and angle-resolved secondary and back-scattered electron yields of conductors via electron and photon excitation.
Year 3: Measurement of NASCAP parameters for existing and newly developed spacecraft materials, and time evolution of secondary electron (SE) and backscattered (BS) yields from environment-induced surface contamination.

For each sample, measurements will be made that will allow determination of all of the 19 parameters used to characterize a material in the current NASCAP database [*Mandell et al*., 1993]. Table 1 identifies each of these parameters, along with the experimental methods and apparatus employed to measure the related physical properties. The measurements are categorized under three headings:

(i) *sample characterization*, used to fully identify the specific materials tested and to allow end users to more accurately assess which material is most closely related to their specific spacecraft materials;
(ii) *conduction related properties*, used to model the response of the materials to accumulated charge; and

(iii) *electron emission* induced by electrons, ions and photons, which determine a material's response to space environment fluxes.

A number of additional measurements, highlighted in italics in column three of Table 1, are intended to provide information which may be incorporated in future versions of engineering tools to enhance the modeling of spacecraft charging. The results of these measurements will be integrated into the databases of current tools and new generation models.

Table 1: Property measurements related to NASCAP modeling parameters.

Property Category	Measured Property (Methods and Apparatus)	Related NASCAP Parameters [(a),(b)]
Sample Characterization	Density (Gravimetric).	Density ρ [9,19].
	Bulk composition (AA, IPC).	Mean atomic number <Z> [4]. Mean atomic weight <A> [10].
	Surface contamination (AES, AES mapping plus UPS, SIMS, EDX, ESD as needed).	
	Surface morphology (*in situ* LEED, SEM; *ex situ* STM, AFM, SEM, optical microscopy).	
	Coating thickness (*in situ* HEED, quartz micro-balance; *ex situ* STM, AFM, optical microscopy).	Dielectric film thickness d [2].
Conduction Related Properties	Dielectric constant (*ex situ* capacitive measurements).	Relative dielectric constant ε_r [1].
	Bulk and surface conductivity (4- point resistance probe measurements).	Bulk conductivity σ_0 [3]. Surface resistivity ρ_s [14]. *Temperature dependence of conductivity*.
	Electrostatic discharge (I-V profiles of non-conducting films on conducting substrates).	Maximum potential before discharge to space V_{max} [15]. Maximum surface potential difference before dielectric breakdown discharge V_{punch} [16].
	High energy plasma-induced conductivity (4-point probe measurements of non-conducting samples for flux of 5-30 keV electrons).	Two parameter fit of radiation-induced conductivity σ_r: k and Δ [17,18].
Electron-induced Emission	BS/SE total yield versus incident electron energy (Emission current from sample for 5 eV to 30 keV monoenergetic electrons using hemi-spherical retarding field analyzer).	Maximum SE yield δ_{max} [5]. Energy for δ_{max}, E_{max} [6]. Parameterless fit for $\eta(E_0)$. *Extended parameter fits for $\delta(E_0)$ and $\eta(E_0)$.* *Incident angle dependence of $\delta(E_0)$ and $\eta(E_0)$.*
	Stopping power data.	4-parameter bi-exponential range law fit for primary electron energy range derived from stopping power data: b_1, n_1, b_2, n_2 [7-10].
	Energy- and angle-resolved BS/SE cross-sections (Energy and angle dependent emission cross-sections using rotatable Faraday cup retarding field analyzer. High resolution energy dependent emission current using HSA or TOF. Monoenergetic electrons from 5 eV to 30 keV.)	*Parameters for BS/SE angular distributions used by NASCAP at various incident energies.* *Deviation from NASCAP BS/SE angular emission distributions.*
Ion-induced Emission	Total electron yield versus incident ion energy (Emission current of biased sample from cold cathode ion guns, 500 eV to 5 keV, or PHI ion guns, 100 eV to 5 keV).	SE yield due to 1 keV proton impact δ^H [11]. Incident proton energy for δ^H_{max} and E^H_{max} [12]. *Energy spectra of emitted electrons.*
Photon-induced Emission	Total electron yield versus incident photon energy (Emission current of biased sample from discharge lamps, 0.5-11 eV, or He resonance lamp, 21.2 and 40.8 eV).	Total electron yield from solar spectrum [13]. *Photon energy dependence of emitted electron yields.*

(a) *Mandell et al.*, 1993.
(b) The numbers of the materials database parameters used in the current version of NASCAP are indicated in square brackets. Proposed additions to the database are indicated in italics.

Facilities and Capabilities

The primary instrument of the USU facility is a standard ultra-high vacuum (UHV) chamber equipped with versatile surface analysis and sample characterization abilities (see Figure 1). This chamber is suitable to simulate diverse space environments including controllable vacuum (< 10^{-10} to 10^{-3} Torr), temperature (<100 to >1500 K), and ambient neutral gases conditions, electron fluxes (four guns with 5 eV to 30 keV mono-energetic sources), ion fluxes (three guns with <0.1 to 5 keV mono-energetic sources for inert and reactive gases), and solar irradiation (two lamps with 0.5 to 11 eV IR/VIS/UV mono-energetic sources; 21.2 and 40.8 eV helium resonance lamp). A variety of detectors are available for property measurements of single or simultaneous electron, ion, and photon, induced emission. These include a standard Faraday cup (FC) detector, hemispherical analyzer (VG VG100AX), cylindrical mirror analyzer (Varian 981-2707), and time of flight (TOF) micro-channel plate detector (Jordan C-0701). Specifically, they allow us to measure total emitted electron (ion) yield, backscattered/secondary yield, and energy spectra. Extensive sample characterization capabilities are also available, including Auger spectroscopy, photoelectron spectroscopy, and secondary ion mass spectroscopy for contamination assessment and scanning electron microscopy, low energy electron diffraction, and *ex situ* scanning tunneling (atomic force) microscopy for morphology examination. Capacitance, conductivity, and electrostatic discharge equipment are available for *ex situ* examination of conduction-related properties.

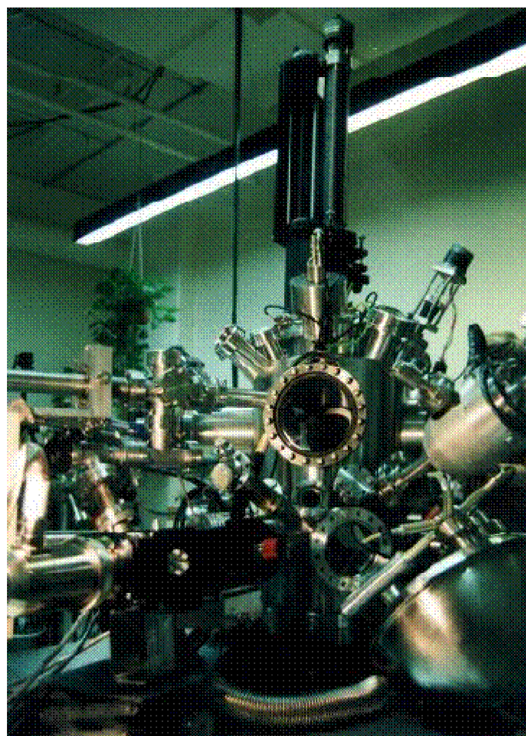

Figure 1. AFOSR ultra-high vacuum surface analysis chamber used for space environment simulation and charged particle scattering studies at Utah State University [*Riffe and Dennison*, 1995].

The facility is also equipped with a second, smaller UHV chamber (shown in Figure 2), dedicated primarily to angle-resolved SE emission measurements. A retarding field analyzer (RFA) Faraday cup type detector [*Nickles et al.*, 1999], continuously rotatable about the sample is used to obtain angle-resolved SE yield and spectra for both normally and obliquely incident electrons in the range of emission angles $-16° < \alpha < +76°$. Angular resolution of the instrument is ~1.5° and the energy resolution is 0.5 eV ± 0.1% of the incident beam energy. The chamber is presently equipped with a 1-3 keV electron source (Varian 981-2454) and a 100-500 eV ion source (Varian 981-2046). In addition to angle-resolved measurements, this chamber is used to study the dynamic evolution of SE yields as a function of surface condition [*Davies and Dennison*, 1997] and sample potential [*Davies and Dennison*, 1999b].

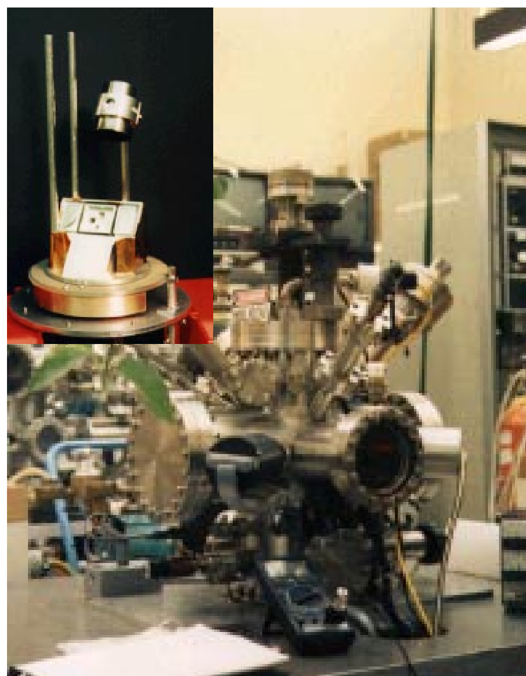

Figure 2. Ultra-high vacuum chamber dedicated to angle-resolved SE measurements and contamination studies. The retarding field analyzer Faraday cup detector, rotating about the sample stage, is shown in inset.

Materials Selected for Study

Based on discussions with spacecraft community specialists and careful consideration, a set of materials for study have been selected to meet two objectives: (1) extending the NASCAP database to include the most common spacecraft materials and (2) investigating representative materials with wide ranges of physical properties. A prioritized list is shown in Table 2.

Table 2: Materials for spacecraft charging studies.

Conducting Materials	
Elemental Metals & Semiconductors	Priority
Al*, Ag*, Au*	1
C (HOPG graphite)	1
a-C (arc evaporated amorphous carbon)	1
Be (sintered)	2
Cu	2
d-C (sputtered diamond-like carbon)	2
a-Si (amorphous), Mg*	2
C (soot)	3
Ge, Ti	3
Alloys	
Al alloy 6061-T6	1
Al alloy 2024-T3	2
Stainless Steel 316, Ti-Al, Al alloy 7075-T6	3
GaAs	3
Al alloy 5667	3
Conductive Coatings	
Aquadag (C)*	3
ITO (vapor deposited In-Sn Oxide)*	3

Insulating Materials	
Bulk Insulators	Priority
Al_2O_3, SiO_2*	1
Kapton*, Teflon*, Mylar	1
Borosilicate glass	2
Kevlar, Nylon	2
BeO, TiO_2	3
Diamond	3
Non-Conductive Coatings	
Irridited Al	2
MgF (Anti-reflection coating)	2
Oxidized Al	2
Anodized Al alloy 6061-T6 (Cr-acid)	3
Anodized Al alloy 5656 (Sulfuric acid)	3
Anodized Mg	3

Specific Spacecraft Materials in Use	
Conductors	Priority
Carbon impregnated Teflon	1
Graphite Al 6061-T61/P120 (4290)	1
Black Kapton conducting thermal control blanket	1
Magnetospheric plasma analyzer (MPA) materials	2
Tether sphere base metal	2
LDEF Al support	3
Insulators	
Carbon fiber composite	1
Graphite cyanate ester P75 tape	1
Graphite epoxy plain weave T300/F263	1
"Yellow" kapton thermal control blanket	1
Fiberglass (antenna material)	2
OSR solar cell coating	2
Solar cell concentrator DC93500	2
Tether sphere painted surface	2
LDEF painted tray	3
LDEF contaminated painted tray	3

Specific Spacecraft Materials under Development	
Conductors	Priority
Other conductive paints	
Other electrically conductive thermal control coatings	2
Insulators	
Al on thermal control blanket	3
AO resistant polymer films & threads	3
ITO on thermal control blanket	3
Other non-conductive paints	
Other graphite composites	
Other optical coatings	
Other solar cell material	2
Other thermal control coatings	2

* Materials characterized in current NASCAP database.

Extended Studies

Our project will also perform a series of investigations to more thoroughly characterize the electronic properties of materials and to enhance the next generation models of spacecraft charging.

The expanded set of materials in the database and the extended incident-energy range of our measurements will allow us to determine which of a number of empirically-based model functions for the reduced SE yield curve provides the best fit to the full data set, particularly in the high energy tail. Figure 3 illustrates this point for four representative functions and typical data. The data can also be used to determine an appropriate model function for the back-scattered yield curve and to improve the modeling of incidence-angle dependence of the SE and backscattered yield curves.

Nickles *et al.* [*Nickles et al.*, 1999] describes initial results of our studies regarding the effects of surface potential on energy-, and angle-resolved SE yields and the need to include these effects in future charging models. A typical angular distribution of argon-sputtered polycrystalline gold is shown in Figure 4 [*Davies*, 1999; *Davies and Dennison*, 1999b]. A parametric fit to the angular-resolved yield using a standard cosine fit (or, additionally, the deviations from such a fit) could prove useful for modeling return current to charged spacecraft surfaces under certain circumstances [*Nickles et al.*, 1999].

Finally, a recent study of the influence of electron stimulated desorption and electron stimulated adsorption of carbon on BS/SE yields from aluminum/aluminum-oxide samples [*Davies and Dennison*, 1997] emphasizes the significance of surface modification (due to, e.g., contamination, surface modification, or changes in surface morphology) on spacecraft charging. Studies are underway to look at similar evolution of BS/SE emission for other sample materials resulting from carbon deposition, organic

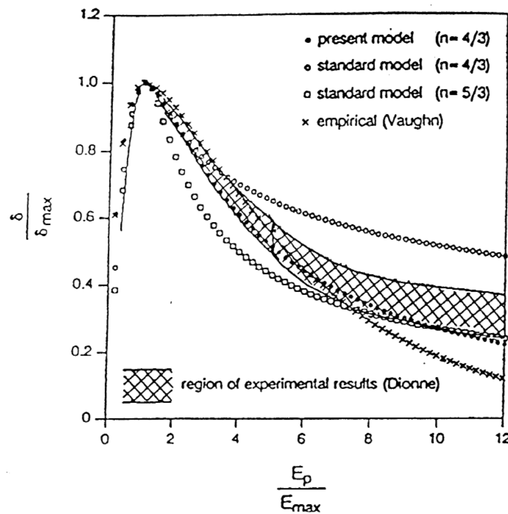

Figure 3. Plot of reduced SE yield curve, $\delta(E_o)/\ \delta_{max}$ vs. E_o/E_{max} [adapted from *Schwartz*, 1990]. The hatched region indicates the extent of typical experimental data [*Dionne*, 1975]. Four theoretical models are shown, (i) Schwartz model with n=4/3 power law (dot), (ii) standard model with n=4/3 power law (circle), (iii) standard model with n=5/3 power law (square), and Vaughn's empirical equation (cross).

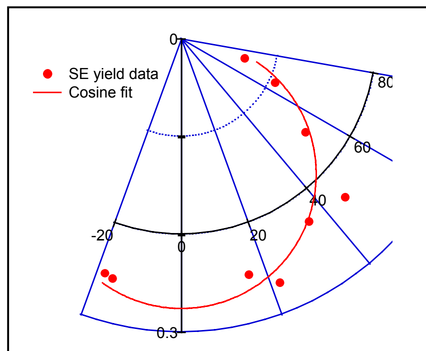

Figure 4. Angle-resolved secondary electron yield of argon sputtered polycrystalline gold at 1500 eV incident energy [*Nickles et al.*, 1999]. The solid line is a cosine fit to the SE yield data of the form $\delta(\theta)=\delta_0 \cdot \cos(\theta)$.

deposition and charging-induced contamination, oxidation, and AO/UV materials degradation.

Acknowledgments. Instrumentation described in this paper was funded through grants from the AFOSR (DURIP) Program and the USU Research Office. The research described here was supported through the NASA/SEE Program, NASA's Graduate Student Researcher's Program (Davies), and fellowships from the NASA Rocky Mountain Space Grant Consortium (Davies, Nickles).

References

Bedingfield, K.L., R.D. Leach, and M.B. Alexander, Spacecraft system failures and anomalies attributed to the natural space environment, NASA Reference Publication 1390, NASA Marshall Space Flight Center, August 1996.

Danilov, V., G. Drolshagen, V.M. Dvoryashin, A.M. Kramarenko, P. Pita Leria, V.S. Sokolov, and Y.V. Vasilyev, Numerical simulation of high-voltage charging at high altitudes: comparison of NASCAP and ECO-M, to appear in the Proceedings of 6th Spacecraft Charging Technology Conference, Boston, MA, 1999.

Davies, R.E., An instrument for experimental secondary electron emission investigations, with application to the spacecraft charging problem, MS Thesis, Utah State University, 1995.

Davies, R.E. and J.R. Dennison, Evolution of secondary electron emission characteristics of spacecraft surfaces, *J. Spacecraft and Rockets*, 34, 4, 571-574, 1997.

Davies, R.E. and J.R. Dennison, Evolution of secondary electron emission characteristics of spacecraft surfaces, to appear in the Proceedings of 6th Spacecraft Charging Technology Conference, Boston, MA, 1999a.

Davies, R.E. and J.R. Dennison, The effect of negative bias on secondary electron emission from spacecraft surfaces, to be submitted to *J. Spacecraft and Rockets*, 1999b.

Davies, R.E., Measurement of angle-resolved secondary electron spectra, Ph.D. Thesis, Utah State University, 1999.

Dennison, J.R., Electronic properties of materials with application to spacecraft charging, NASA Space Environments and Effects Program Grant, 7/1998-7/2001.

Dionne, G.F., Origin of secondary-electron-emission yield-curve parameters, *J. Appl. Phys*., 46, 8, 3347-3351, 1975.

Hastings, D. and H. Garrett, Spacecraft-environment interactions, Cambridge University Press, 1996.

Heynderickx, D., B. Fontaine, B. Quaghebeur, W.C. Carey, and E.J. Daly, SPENVIS: ESA's space environment information system and models for spacecraft charging, to appear in the Proceedings of 6th Spacecraft Charging Technology Conference, Boston, MA, 1999.

Leach, R.D. and M.B. Alexander, Failures and anomalies attributed to spacecraft charging, NASA Reference Publication 1375, NASA Marshall Space Flight Center, August 1995.

Mandell, M.J., P.R. Stannard, and I. Katz, NASCAP programmer's reference manual, NASA Lewis Research Center, May 1993.

Mandell, M.J., I. Katz, and D.L. Cooke, Toward a more robust spacecraft charging algorithm, to appear in the Proceedings of 6th Spacecraft Charging Technology Conference, Boston, MA, 1999.

Nickles, N., R.E. Davies, and J.R. Dennison, Energy-angle-resolved secondary electron cross sections and applications to spacecraft charging, to appear in the Proceedings of 6th Spacecraft Charging Technology Conference, Boston, MA, 1999.

Riffe, D.M. and J.R. Dennison, Ultra-high vacuum electron scattering chamber for the characterization of materials in severe environments: surface and nanocrystalline solids, DOD-Defense University Research Instrumentation Grant, 8/1995-7/1996.

Schwarz, A., Application of a semi-empirical sputtering model to secondary electron emission, *J. Appl. Phys*., 68, 5, 2382, 1990.